Supporting information

Bio-waste chitosan-derived N-doped CNT supported Ni-nanoparticles for selective hydrogenation of nitroarenes

*Jacky H. Advani,[a,b] Krishnan Ravi,[a,b] Dhanaji R. Naikwadi,[a,b] Hari C. Bajaj,[a,b] and Ankush V. Biradar [a,b,]**

[a]Inorganic Materials and Catalysis Division, CSIR-Central Salt and Marine Chemicals Research Institute (CSIR-CSMCRI), G. B. Marg, Bhavnagar-364002, Gujarat, India.
E-mail: ankush@csmcri.res.in

[b]Academy of Scientific and Innovative Research (AcSIR), Ghaziabad-201002, Uttar Pradesh, India.

Contents

S1. Materials and methods

Raw Materials

Chitosan, 4-ethylnitrobenzene was purchased from TCI Chemicals, India. Hydrochloric acid (HCl; 35.4%), 4-chloronitrobenzene, Nitrobenzene were purchased from S. D. Fine Chemicals, India. 4-methyl nitrobenzene, 4-nitroaniline were purchased from SRL, India. 4-cyanonitrobenzonitrile, 4-nitrobenzensulfonamide, 1-nitronaphthalene, 1,4-dinitrobenzene, 4-nitrobenzaldehyde, 5-nitroindole and 4-chloro-β-nitrostyrene were obtained from Sigma-Aldrich. All the reagents were used without any further purification.

Material Characterizations

The structural characterization studies of the catalyst were carried out by different physiochemical methods. The PXRD analysis was carried out using Philips X'pert MPD system for powder X-ray Diffractometer. The black powder obtained was scanned in the range of 10-80° using CuKα radiation of 1.54056 Å wavelength with a Ni filter. A Perkin-Elmer GX spectrophotometer was used for the Fourier-transform infrared spectrophotometry (FTIR) spectra using KBr pellets in the wavelength range of 400-4000 cm^{-1}. The total concentration of metal was determined by inductively coupled plasma optical emission spectrometry (ICP-OES) (Perkin Elmer, Optima 2000) by completely digesting the material in aqua regia. The reducibility of the precursor was analyzed by the temperature programmed reduction (TPR), and the total basicity of the catalyst was evaluated by temperature programmed desorption (TPD) using Micromeritics Analyzer, AutoChem-II 2920 with a continuous flow system. The sample was subjected to thermal activation under helium at 250 °C for 4 h. The stabilization of the sample was done under 10% of H_2/Ar, and the TPR profiles were obtained by heating at the rate of 10 °C min^{-1} from room temperature to 400 °C. The saturation was obtained by using a mixture of 10% CO_2/He and the TPD profile was obtained by heating at a rate of 10 °C min^{-1} from 90 °C to 800 °C. Raman spectroscopic analysis of the catalyst was done with 532 nm argon source laser excitation with 10 mW power in the range of 1000-2000 cm^{-1}. The energy dispersive X-ray (EDX) mapping and morphology of the catalyst was determined using a JEOL JSM 7100F field emission scanning electron microscope (FE-SEM). The synthesized catalyst was dispersed in isopropyl alcohol by sonication and was drop casted on a brass stub. The stub was dried under vacuum and used for analysis. Transmission electron microscope (TEM) (JEOL JEM 2100) was used to analyse the size and shape of the particles and recording the selected area electron diffraction (SAED) of the sample. The samples were loaded on the TEM

grid by dispersing it in isopropyl alcohol using ultrasonicator and then drop casting the suspension on the TEM grid. This drop casted grid was dried in a vacuum oven prior to analysis. X-ray photoelectron spectroscopy (XPS) was performed using an ESCA+ (Omicron Nanotechnology, Germany) with a monochromatized Al-Kα X-ray (hν = 1486.7 eV) as the excitation source (15 kV and 20 mA). The pass energy for the survey spectrum was 50 eV and 20 eV in case of the short scan. The sample was placed on the copper tape and degassed in the XPS FEL chamber to minimize the air contamination. A charge neutralizer of 2 keV was used to overcome any charging problem, and the calibration was done using the adventitious C1s feature at 284.6 eV as a reference. All the spectra's were recorded at 90° of the X-ray source. The ^{1}H and ^{13}C spectra were recorded on Bruker, Avance II (600MHz). The NMR Chemical shifts were recorded in $CDCl_3$ or DMSO-d_6 solutions referenced to tetramethylsilane (TMS) (0.00 ppm) or $CDCl_3$ (7.26 ppm) and DMSO- d_6 (2.50 ppm) for ^{1}H NMR and $CDCl_3$ (77 ppm) and DMSO- d_6 (39.5 ppm) for ^{13}C NMR.

Product Analysis

The products were analyzed by gas chromatography (Agilent GC 7890B) equipped with HP-5 capillary column of 30 m x 0.250 mm x 0.25 µm dimension and a FID detector and GC-MS (Shimadzu, GC-MS QP 2010, Japan). The reproducibility of the results was ensured by repeated experiments under identical conditions and was found to be consistent with ± 5% variation.

GC-MS data for the products

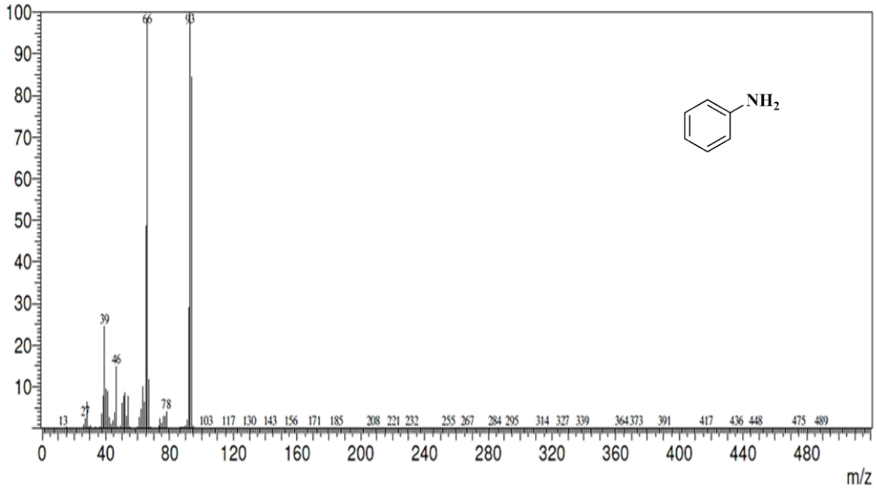

Figure S1. GC-MS profile of aniline.

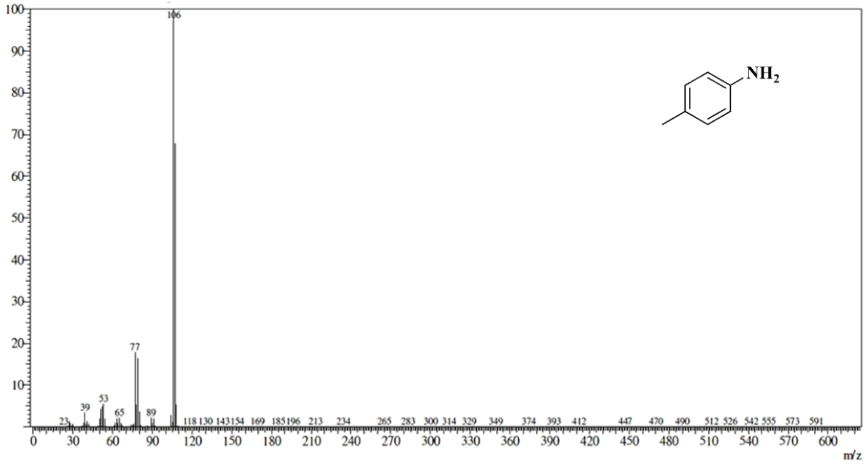

Figure S2. GC-MS profile of *p*-toluidine

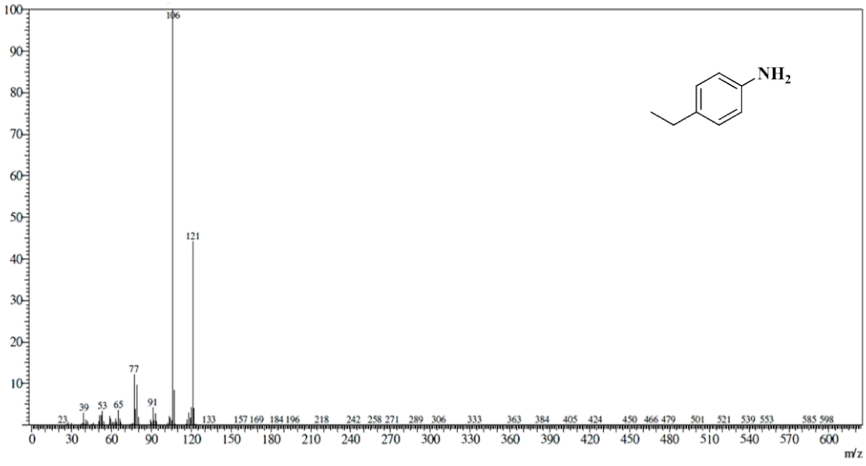

Figure S3. GC-MS profile of 4-ethylaniline

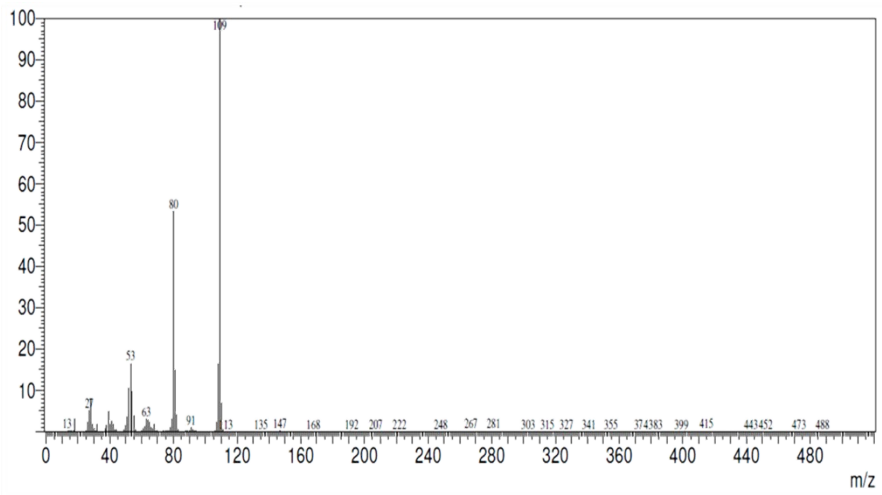

Figure S4. GC-MS profile of 4-aminophenol

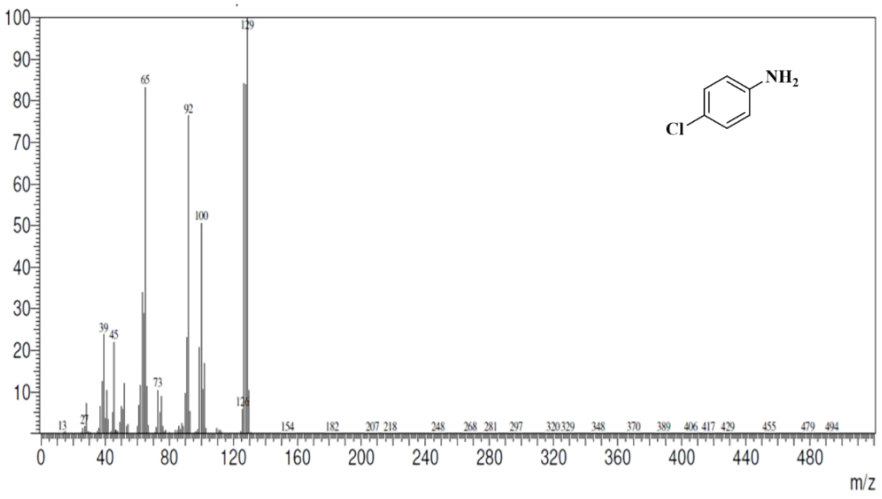

Figure S5. GC-MS profile of 4-chloroaniline

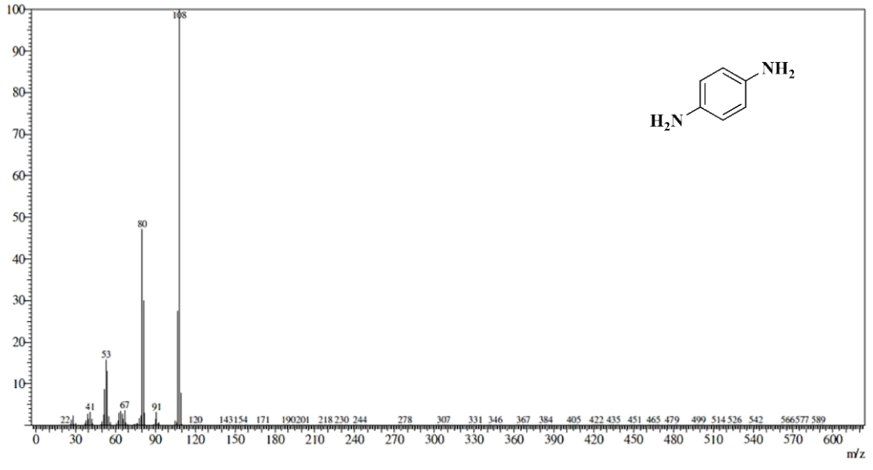

Figure S6. GC-MS profile of Benzene-1,4-diamine (*p*-phenylene diamine)

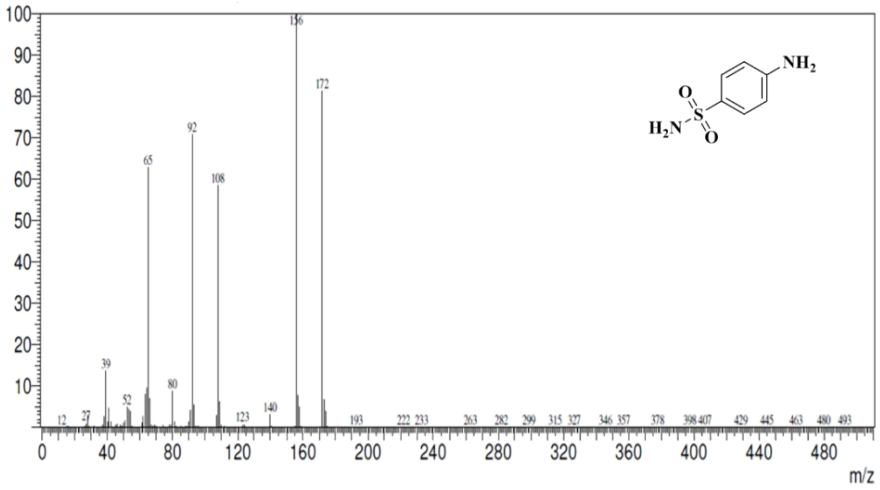

Figure S7. GC-MS profile of 4-aminobenzenesulfonamide (Sulphanilamide)

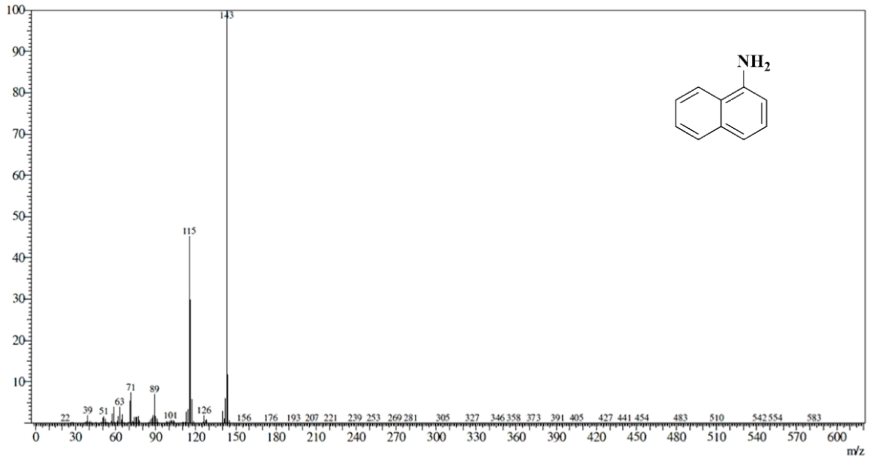

Figure S8. GC-MS profile of 1-naphthylamine

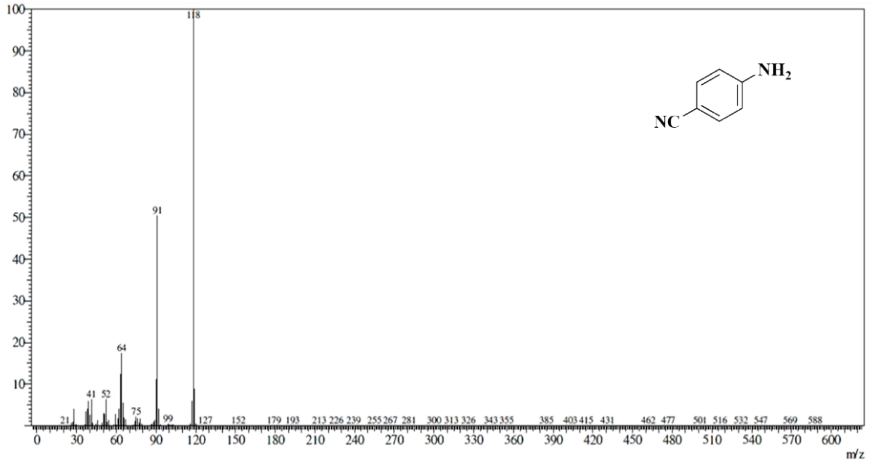

Figure S9. GC-MS profile of 4-aminobenzonitrile

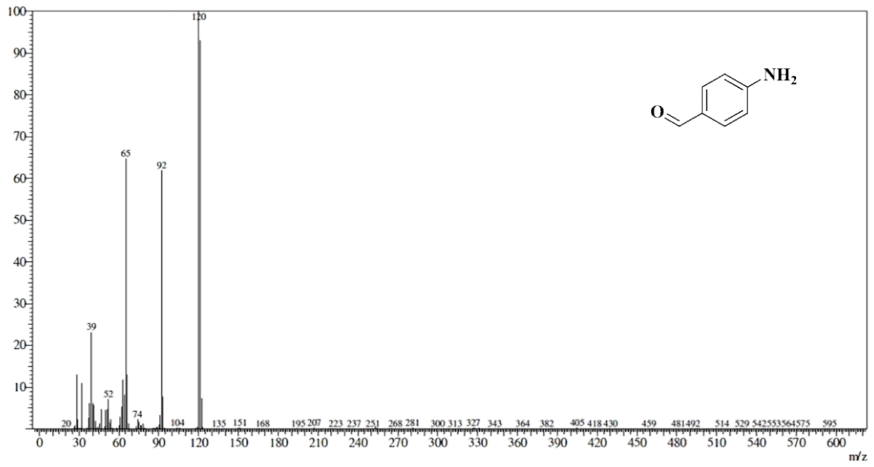

Figure S10. GC-MS profile of 4-aminobenzaldehyde

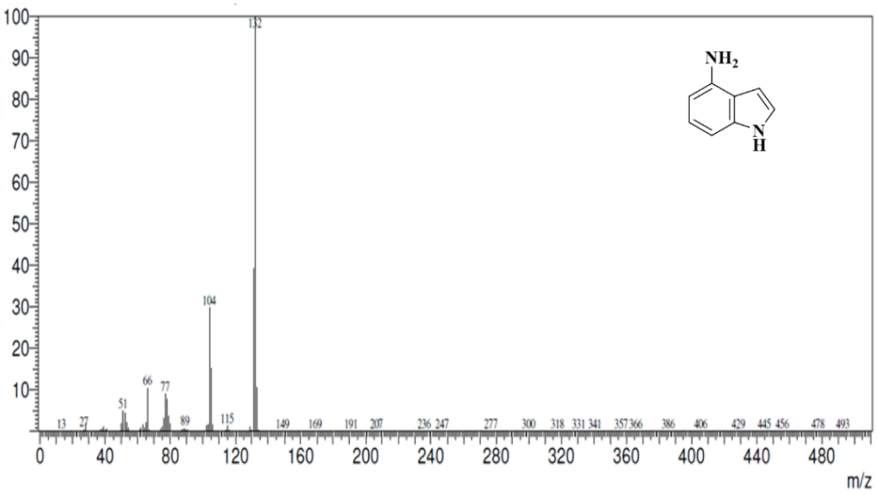

Figure S11. GC-MS profile of 4-amino-1H-indole

Figure S12. GC-MS profile of Sulphanilamide.

S3. Recyclability chart for Ni@N-CNT nanocatalyst

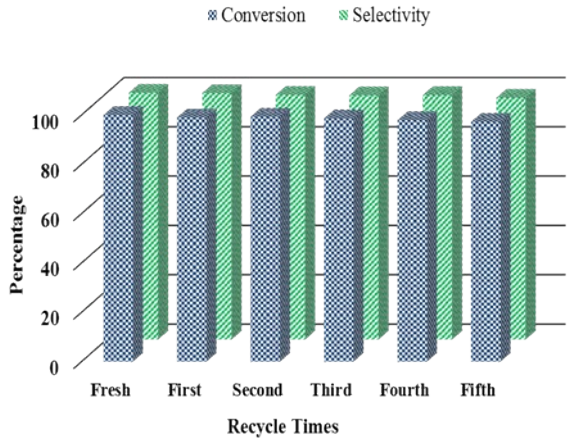

Figure S13. Recyclability data chart: 2 mmol nitrobenzene, 50 mg Ni@N-CNT, 20 mL methanol, 5 bar H_2, 80 °C and 800 rpm.

S4 ^{1}H and ^{13}C NMR spectra of some isolated products

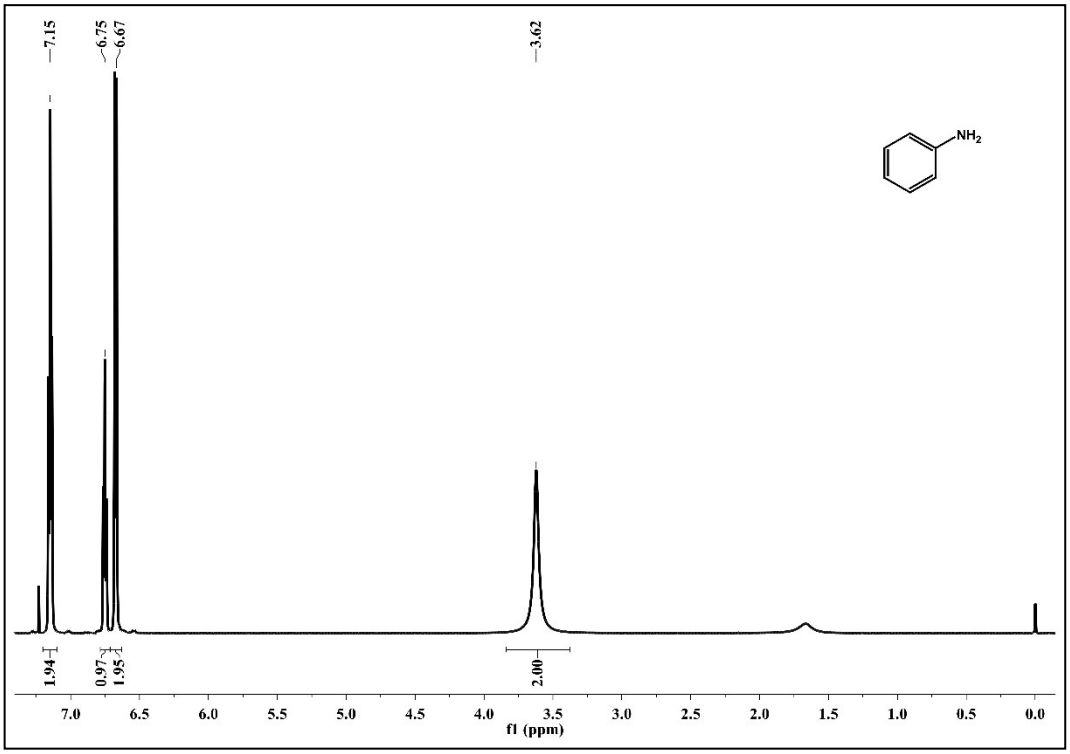

Figure S14. ^{1}H NMR of aniline.

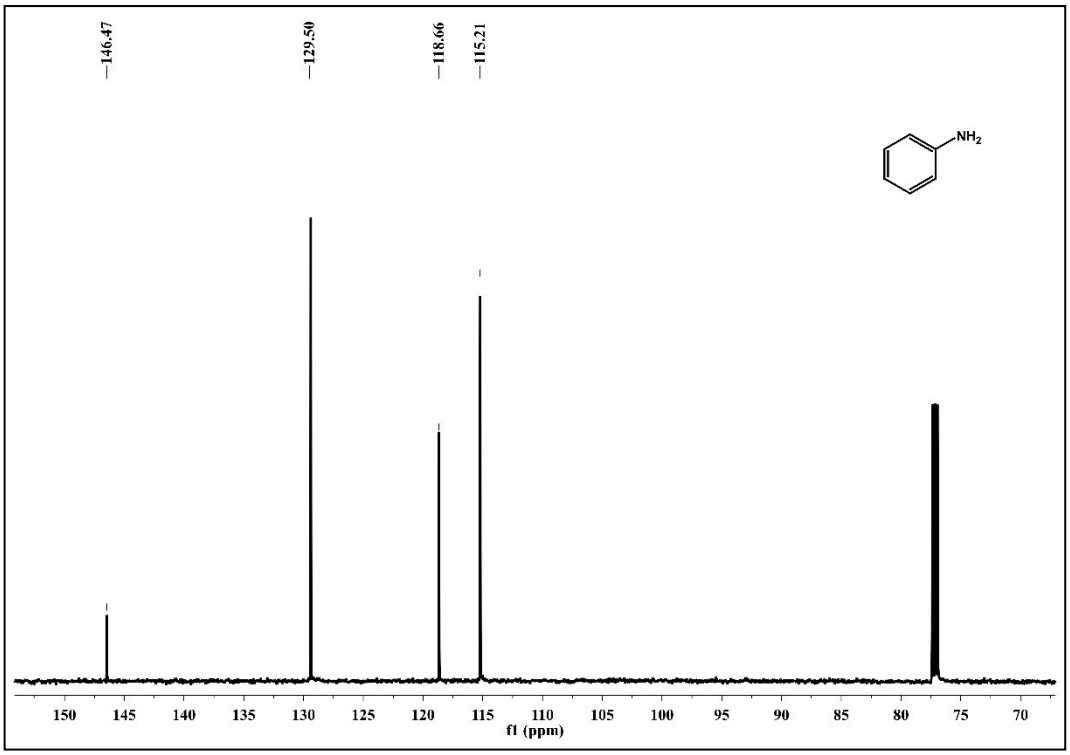

Figure S15. ^{13}C NMR of aniline.

^{1}H NMR (600 MHz, $CDCl_3$) δ 7.15 (t, 2H), 6.75 (t, 2H), 6.67 (d, 2H), 3.62 (s, 2H) **^{13}C NMR** (150 MHz, $CDCl_3$) δ 146.5, 129.5, 118.7, 115.2

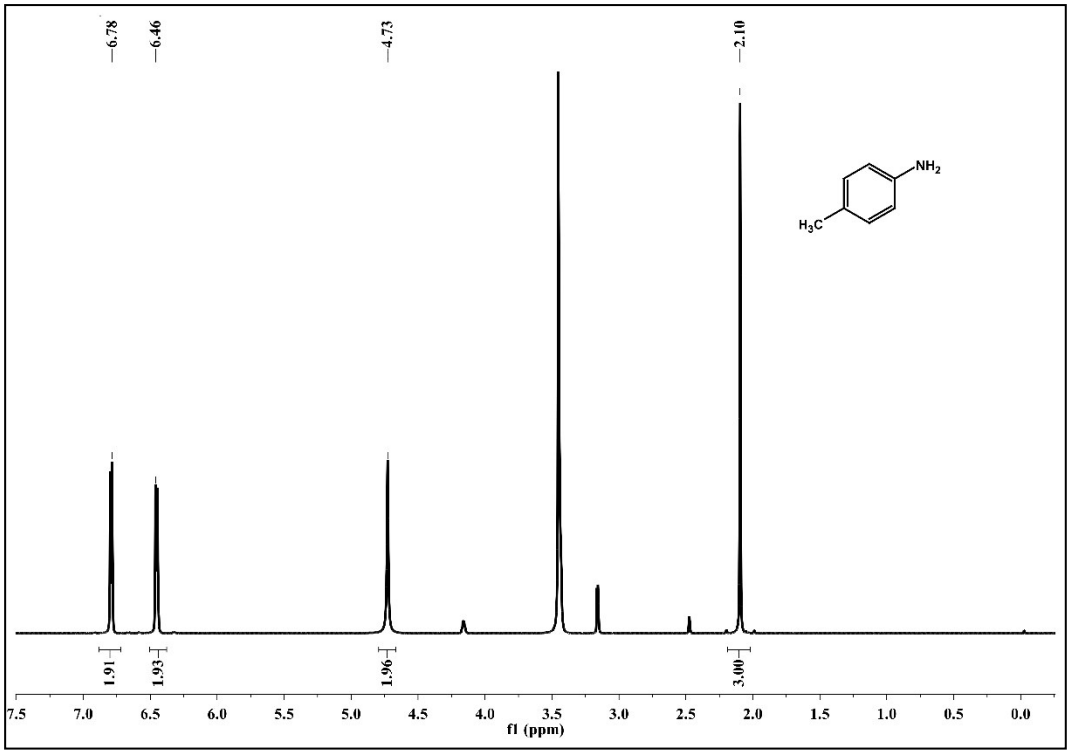

Figure S16. ^{1}H NMR of *p*-toludine.

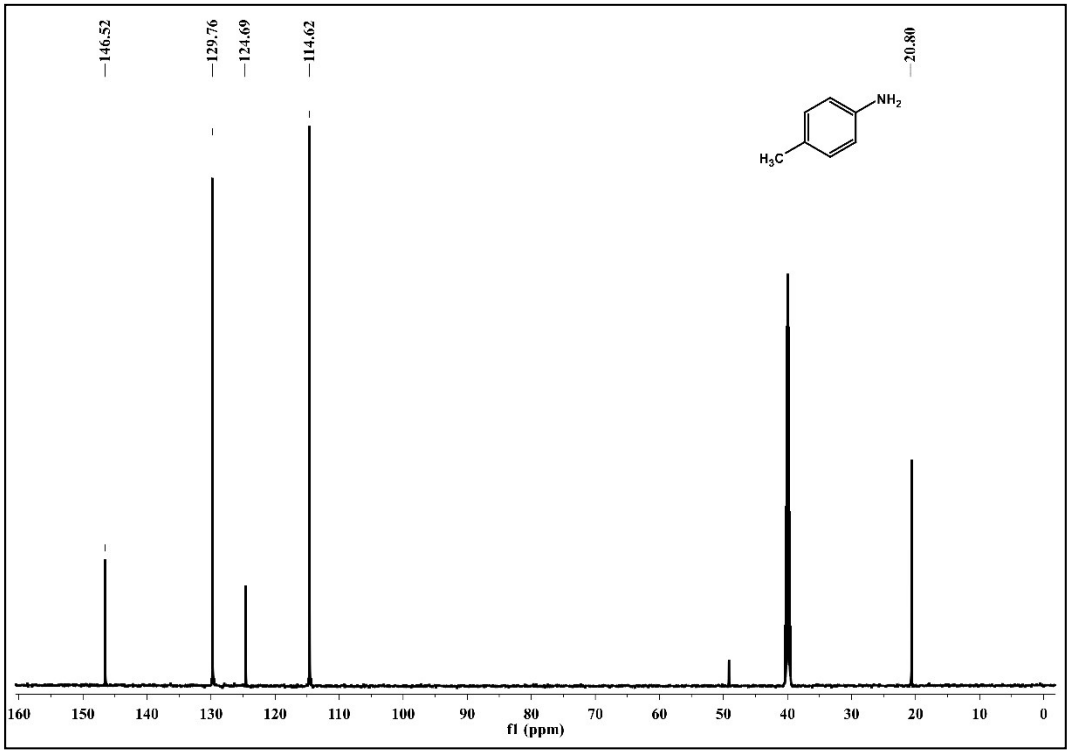

Figure S17. ^{13}C NMR of *p*-toludine.

^{1}H NMR (600 MHz, DMSO-d_6) δ 6.78 (d, 2H), 6.46 (d, 2H), 4.73 (s, 2H), 2.10 (s, 3H). **^{13}C NMR** (150 MHz, DMSO-d_6) δ 146.5, 129.8, 124.7, 114.6, 20.8

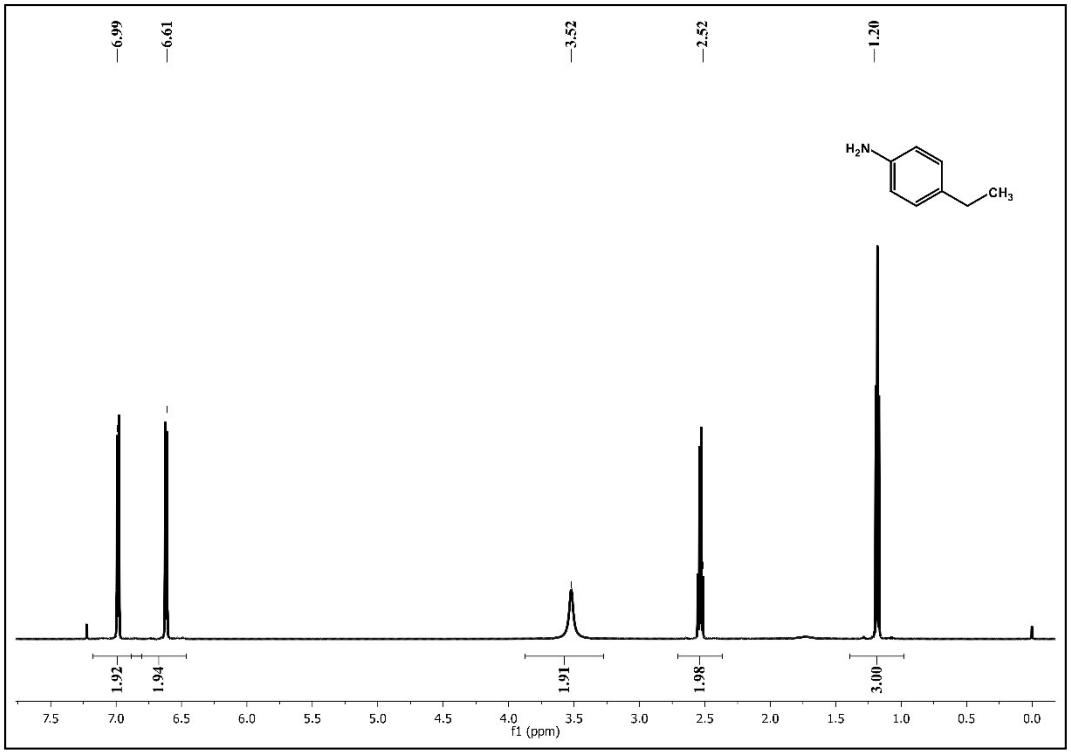

Figure S18. ^{1}H NMR of 4-ethylaniline.

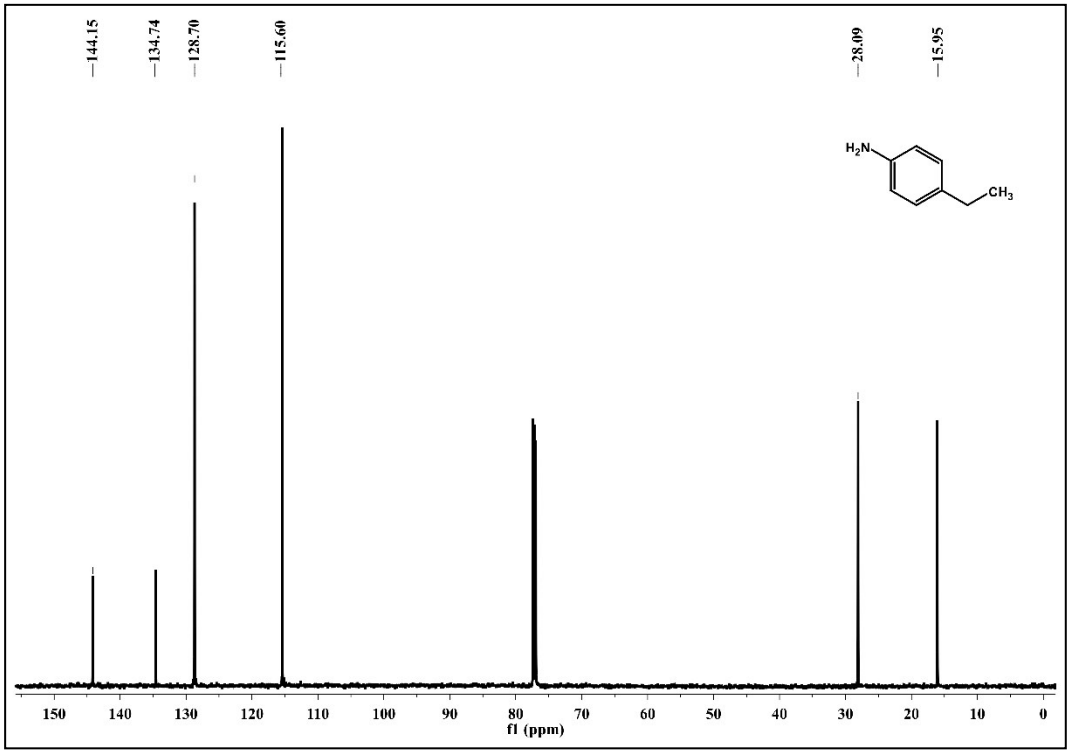

Figure S19. ^{13}C NMR of 4-ethylaniline.

^{1}H NMR (600 MHz, $CDCl_3$) δ 6.99 (d, 2H), 6.61 (d, 2H), 3.52 (s, 2H), 2.52 (q, 2H), 1.20 (t, 3H). **^{13}C NMR** (150 MHz, $CDCl_3$) δ 144.2, 134.7, 128.7, 115.6, 28.09, 15.9

Figure S20. ^{1}H NMR of 1-aminonapthalene.

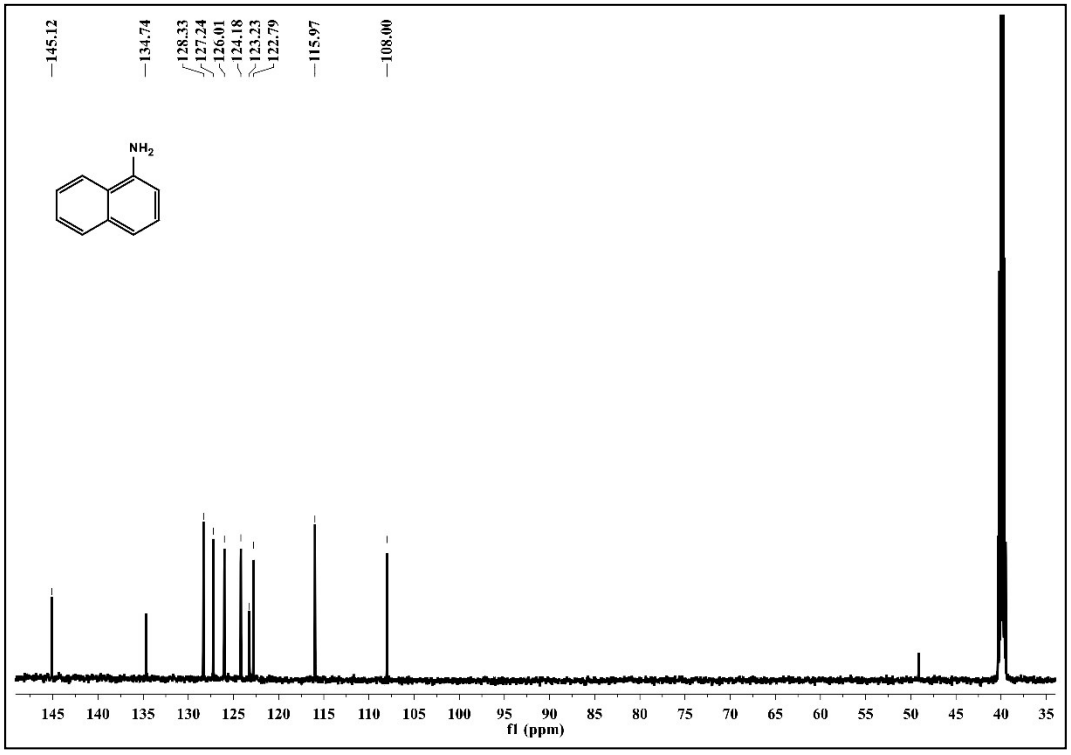

Figure S21. ^{13}C NMR of 1-aminonapthalene.

^{1}H NMR (600 MHz, $CDCl_3$) δ 8.06 (d, 1H), 7.72 (d, 1H), 7.40 (t, 1H), 7.36 (t, 1H), 7.20 (t, 1H), 7.09 (d, 1H), 6.69 (d, 1H), 5.68 (s, 2H). **^{13}C NMR** (150 MHz, $CDCl_3$) δ 145.1, 134.7, 128.3, 127.2, 126.0, 124.2, 123.2, 122.8, 116.0, 108.0

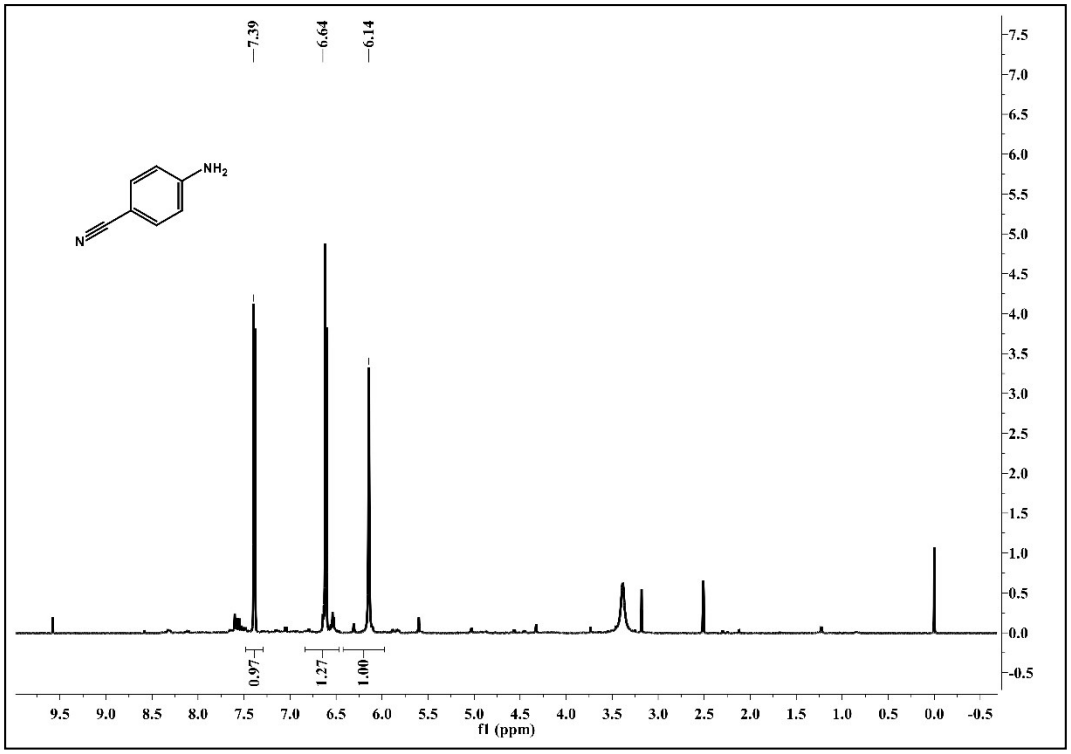

Figure S22. ^{1}H NMR of 4-aminobenzonitrile.

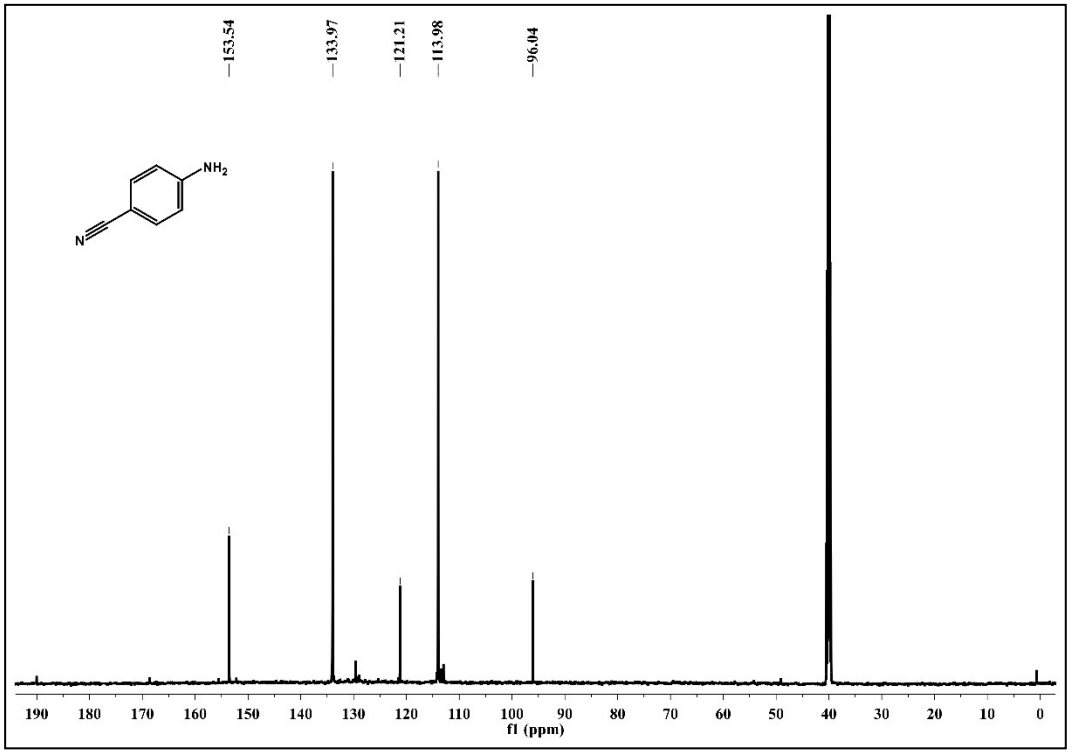

Figure S23. ^{13}C NMR of 4-aminobenzonitrile.

^{1}H NMR (600 MHz, $CDCl_3$) δ 7.39 (d, 2H), 6.64 (d, 2H), 6.14 (s, 2H). **^{13}C NMR** (150 MHz, $CDCl_3$) δ 153.5, 134.0, 121.2, 114.0, 96.0